INSTITUTE OF PHYSICS PUBLISHING MODELLING AND SIMULATION IN MATERIALS SCIENCE AND ENGINEERING

Modelling Simul. Mater. Sci. Eng. **10** (2002) 673–684 PII: S0965-0393(02)40125-8

Approximate solutions to three-dimensional unsteady heat conduction through plane flaws within anisotropic media using a perturbation method

A Bendada

Industrial Materials Institute, National Research Council, 75 De Mortagne Boulevard, Boucherville, QC, Canada J4B 6Y4

Received 13 May 2002, in final form 30 July 2002
Published 2 September 2002
Online at stacks.iop.org/MSMSE/10/673

Abstract

This paper studies the analytical solution of three-dimensional thermal conduction in an anisotropic medium containing one or several plane flaws. This problem is typical of one or several delaminations within a composite material. The method proposed here consists in applying a Laplace transform on the time variable followed by a Fourier integral transform on space variables (Cartesian geometry). The numerical or semi-analytical true solutions for the integral equations generated by this problem may be very time consuming, especially in a three-dimensional configuration. Therefore, we suggest a modelling reduction using a first order analytical perturbation method, which is subsequently improved by applying Padé's approximant approach. The latter formalism leads to a better tracking of the true solution and increases the validity field of the perturbed approximation.

1. Introduction

In recent years, the study of laminated composites has been of great interest in applied science and engineering owing to their widespread use in various industrial fields (aerospace, nuclear, microelectronics, etc). The complex processes used in the manufacture of such materials, increase the risk of flaw appearance, whose consequences may be crucial under service conditions. In most cases, the control has to be nondestructive in order to allow inspection during the different stages of the part's life. For quality control purposes, methods based on heat transfer may be very effective [1]. Stimulated infrared thermography is one of the alternatives that may be applied for flaw detection. In this technique, the composite slab is radiated by a uniform heat pulse on one face while the transient temperature, either on the same face or on the opposite one, is recorded using an infrared camera. The temperature difference, between the pixel of interest on the infrared frame and on a reference area considered to be sound on the same frame, represents a signature of the subsurface flaw. It is this signal, usually called the contrast thermogram, which is commonly used to detect and quantify the flaw.

The discontinuity characterization is carried out using the contrast as an input to an inverse algorithm. To accurately identify the features of the discontinuity, three stages have to be considered. The first step is to develop a forward model describing the contrast field evolution in a mathematical formalism as accurately, simply and rapidly as possible. The following step is to conceive a measurement procedure which outputs the most correct and less noisy signal. The last step is to develop an inverse problem that estimates the unknown parameters in such a way that the deviation between the experimental data and the forward problem is minimized [2–4]. In this work, we focus only on the forward modelling of heat transfer through a two-dimensional plane flaw. Inverse procedures are not considered here. Interested readers are referred to reference [5] where a typical inverse treatment based on similar solutions has been dealt with.

The simulation of heat transfer in a material containing a discontinuity of finite size requires either a numerical approach [6–7], a semi-analytical approach [8–10] or an analytical approach [5, 9–16]. This problem is particularly difficult to solve by numerical means since it requires a very high density mesh near the front face and the vicinity of the discontinuity where thermal gradients are expected to be high. Furthermore, analytical modelling may be very effective not only in calculation time but also in identifying the discontinuity parameters and analysing their influence on the thermal contrast.

This work emphasizes the use of a modified perturbation method to simulate the forward problem. The perturbation approach is based on an asymptotic expansion of the physical field (temperature or heat flux) versus a small parameter intervening in the model [17–19]. The approach has already been used to simulate heat diffusion through a one-dimensional flaw providing the assumption of weak thermal resistance R_c (the small parameter) [5, 9–10]. When the resistance is high, a large number of terms of the expansion series are needed for the convergence and the algorithm becomes as slow as the numerical methods. To keep its fast calculation advantage, we suggest carrying out the perturbation expansion only up to its first order and afterwards enhance the solution using Padé's approximants [20, 21]. The results are simple, and valid even for high resistances. An extension of the solution to describe the heat transfer through several superimposed flaws (e.g. a multi-delamination in an impacted composite [9, 14]) or through a continuously non-uniform resistance $R_c(x, y)$ (e.g. a non-uniform adhesive film between two plates [9, 11, 12, 15]) is also presented.

In the second part of this work, we apply the perturbation method to a flaw whose thermal resistance is very high. Now, the small parameter is the conductance $(1/R_c)$. Following the same methodology as the one for small resistances, we developed a simple solution which is valid for any value of the thermal resistance and also equivalent to the solution found for small resistances.

2. Formulation of the problem using quadrupoles

The case of a rectangular $(L \times l)$ flat slab of thickness e that contains a resistive flaw of finite width a and finite length b, with a uniform contact resistance R_c on its whole area, is typical of a delamination in a composite stratified material (figure 1). It is assumed that the thermal excitation of the slab is a Dirac heat pulse characterized by a uniform absorbed energy by unit area Q (at time $t = 0$) on the front face ($z = 0$). The slab is insulated from the outside and the material temperature is zero before excitation. Since only the face temperatures are of interest, the quadrupole technique is the easiest formalism to be implemented [10, 16]. The concept is to apply a Laplace transform on the time variable and a Fourier transform (Cartesian geometry) on the space variables [22–25]. Heat transfer modelling of multi-layer materials is then reduced to a simple multiplication of matrices in the transformed domain.

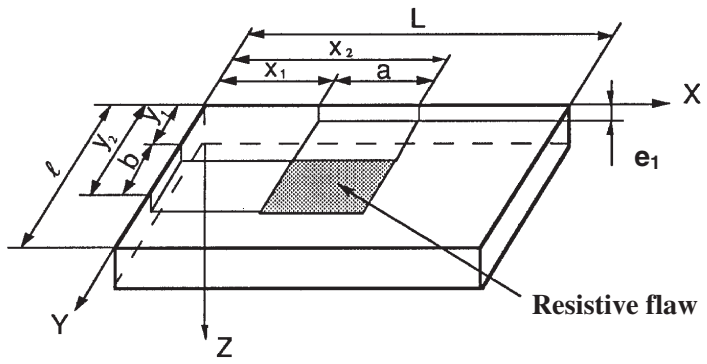

Figure 1. Geometric sketch of a finite extent flaw within an anisotropic material: e_1 = flaw depth; e = total thickness; a = flaw length; b = flaw width; L = specimen length; l = specimen width; z = direction of the heating radiation; x_1, x_2, y_1, y_2 = flaw border coordinates.

The Laplace transform $\tau(x, y, z, p)$ (Laplace variable p) of temperature $T(x, y, z, t)$ in the specimen is the solution of the following set of equations

$$\frac{\partial^2\tau}{\partial z^2} + \frac{\lambda_x}{\lambda_z}\frac{\partial^2\tau}{\partial x^2} + \frac{\lambda_y}{\lambda_z}\frac{\partial^2\tau}{\partial y^2} - \frac{p}{a_z}\tau = 0 \tag{1a}$$

$$x = 0, L \;\rightarrow\; \frac{\partial\tau}{\partial x} = 0 \tag{1b}$$

$$y = 0, l \;\rightarrow\; \frac{\partial\tau}{\partial y} = 0 \tag{1c}$$

$$z = 0 \;\rightarrow\; -\lambda_z\frac{\partial\tau}{\partial z} = Q \tag{1d}$$

$$z = e_1 \;\rightarrow\; \frac{\partial\tau^{\sup}}{\partial z} = \frac{\partial\tau^{\inf}}{\partial z} \tag{1e}$$

$$\tau^{\sup} - \tau^{\inf} = R_c s(x, y)\left[-\lambda_z\frac{\partial\tau}{\partial z}\right] \tag{1f}$$

$s(x, y) = 1$ if $(x, y) \in \{[x_1, x_2] \times [y_1, y_2]\}$ and $s(x, y) = 0$ elsewhere; superscripts sup and inf relate to the upper and lower side of the flaw.

$$z = e \;\rightarrow\; \frac{\partial\tau}{\partial z} = 0 \tag{1g}$$

The analysis can be simultaneously performed for both isotropic and anisotropic (provided that the slab faces are parallel to the principle directions of anisotropy) materials by using the following dimensionless governing parameters:

$$\tau^* = \frac{\tau}{Qe/\lambda_z} \qquad a^* = \frac{a}{e}\left(\frac{\lambda_z}{\lambda_x}\right)^{1/2} \qquad \psi^* = \frac{\psi}{Q}$$

$$b^* = \frac{b}{e}\left(\frac{\lambda_z}{\lambda_y}\right)^{1/2} \qquad x^* = \frac{x}{e}\left(\frac{\lambda_z}{\lambda_x}\right)^{1/2} \qquad p^* = \frac{e^2 p}{a_z}$$

$$y^* = \frac{y}{e}\left(\frac{\lambda_z}{\lambda_y}\right)^{1/2} \qquad R_c^* = \frac{R_c}{e/\lambda_z} \qquad z^* = \frac{z}{e} \qquad e_1^* = \frac{e_1}{e}$$

ψ is the Laplace transform of the z component of the heat flux density $\varphi(=-\lambda_z \partial T/\partial z)$. In the remaining text the asterisk superscript will be omitted for simplicity reasons. The partial differential equation (1a) then becomes

$$\frac{\partial^2 \tau}{\partial z^2} + \frac{\partial^2 \tau}{\partial x^2} + \frac{\partial^2 \tau}{\partial y^2} - p\tau = 0 \tag{2}$$

Applying the Fourier transform to the function $\tau(x, y, z, p)$ and based on the lateral boundary conditions [9], a cosine type is used:

$$\theta(\alpha, \beta, z, p) = \int_0^L \int_0^l \tau(x, y, z, p) \cos(\alpha x) \cos(\beta y)\, \mathrm{d}x\, \mathrm{d}y \tag{3}$$

The boundary conditions on the opposite faces, $x = L$ and $x = l$, determine the discrete values allowed for the space frequencies: $\alpha_j = j\pi/L$, $\beta_k = k\pi/l$; where j and k are non-negative integers.

Using equation (3) and the lateral boundary conditions, the heat equation (2) yields

$$\frac{\partial^2 \theta}{\partial z^2} - (p + \alpha^2 + \beta^2)\theta = 0 \tag{4}$$

If Φ is the Fourier transform of the Laplace heat flux density Ψ, which is unity at $z = 0$ and zero at $z = 1$ (equations (1d) and (1g)), we obtain

$$z = 0 \;\rightarrow\; \Phi(\alpha, \beta, 0, p) = \frac{\sin(\alpha L)}{\alpha} \frac{\sin(\beta l)}{\beta} \tag{5}$$

$$z = 1 \;\rightarrow\; \Phi(\alpha, \beta, 1, p) = 0 \tag{6}$$

The solution of equation (7) has the following form:

$$\theta = F \cosh(uz) + G \sinh(uz) \qquad u = \sqrt{p + \alpha^2 + \beta^2} \tag{7}$$

If the arguments other than z are omitted in the Laplace–Fourier transforms θ and Φ, this equation leads to a linear relationship between the two quantities on the front ($z = 0$) and rear ($z = 1$) faces:

$$\theta(0) = A\,\theta(1) + B\,\Phi(1) \tag{8a}$$

$$\Phi(0) = C\,\theta(1) + D\,\Phi(1) \tag{8b}$$

Boundary conditions (1d)–(1g) can be rewritten under the following matrix forms commonly called quadrupoles [10, 16]:

$$\begin{bmatrix} \theta(0) \\ \dfrac{\sin(\alpha L)}{\alpha} \dfrac{\sin(\beta l)}{\beta} \end{bmatrix} = \begin{bmatrix} A_1 & B_1 \\ C_1 & D_1 \end{bmatrix} \begin{bmatrix} \theta^{\sup} \\ \Phi(e_1) \end{bmatrix} \tag{9a}$$

$$\begin{bmatrix} \theta^{\sup} \\ \Phi(e_1) \end{bmatrix} = \begin{bmatrix} \theta^{\inf} + R_c I \\ \Phi(e_1) \end{bmatrix} \tag{9b}$$

$$\begin{bmatrix} \theta^{\inf} \\ \Phi(e_1) \end{bmatrix} = \begin{bmatrix} A_2 & B_2 \\ C_2 & D_2 \end{bmatrix} \begin{bmatrix} \theta(1) \\ 0 \end{bmatrix} \tag{9c}$$

where

$$I = \int_{x_1}^{x_2} \int_{y_1}^{y_2} \psi(x, y, e_1, p) \cos(\alpha x) \cos(\beta y)\, \mathrm{d}x\, \mathrm{d}y \tag{9d}$$

$A_i = D_i = \cosh(ue_i)$, $B_i = (1/u)\sinh(ue_i)$, $C_i = u \sinh(ue_i)$ for $i = 1, 2$; e_1 and e_2 are the thicknesses of the two layers of the specimen.

A true solution of equations (9) can be found if the heat flux at the interface $\Phi(e_1)$ is known. Fourier components of the latter are obtained by solving a linear set of equations. This set is

generated by substituting the Laplace heat flux $\Psi(e_1)$ in the integral I of equation (9d) by the inverse Fourier series allowing its calculation from a given $\Phi(e_1)$. Details on this procedure as well as illustration examples in a two-dimensional geometry can be found elsewhere [9, 10]. In some cases, this method may be CPU intensive to converge, particularly in a three-dimensional analysis. As an economic alternative, in the next paragraph, we present a more rapid method to solve the same problem, namely, the perturbation method [17–19].

3. Formulation of the problem using perturbations

The perturbation method consists in writing asymptotic series expansions of the variables θ and Φ with respect to a small parameter in the model. These series expansions are then introduced into equations (9) and a term-by-term identification of the coefficients of the successive powers of the small parameter leads to a coupled series of linear sets. These sets allow the calculation of the different components θ_i and Φ_I. In the following sections, we will focus on the cases where the thermal resistance of the flaw is very small and very high, respectively.

3.1. Flaw of small resistance

The asymptotic series expansions with respect to the small parameter R_c that will be denoted ε (for clarity reasons) from now on are

$$\theta(\alpha, \beta, z, p) = \sum_{i=0}^{\infty} \theta_i(\alpha, \beta, z, p)\varepsilon^i \tag{10a}$$

$$\Phi(\alpha, \beta, z, p) = \sum_{i=0}^{\infty} \Phi_i(\alpha, \beta, z, p)\varepsilon^i \tag{10b}$$

Term by term identification of the coefficients of ε^n leads to the following quadrupole equations.

3.1.1. ε^0 order identification. For zero order, equations (9) result in

$$\begin{bmatrix} \theta_0(0) \\ \dfrac{\sin(\alpha L)}{\alpha}\dfrac{\sin(\beta l)}{\beta} \end{bmatrix} = \begin{bmatrix} A_1 & B_1 \\ C_1 & D_1 \end{bmatrix}\begin{bmatrix} A_2 & B_2 \\ C_2 & D_2 \end{bmatrix}\begin{bmatrix} \theta_0(1) \\ 0 \end{bmatrix} \tag{11}$$

This zero order term represents the one-dimensional heat transfer within a flawless plate. As we will further see, the perturbation analysis requires that the zero order Laplace flux be known within the flawless plate at the flaw depth. Therefore, the zero order Laplace flux can be extracted from equation (11):

$$\psi_0(e_1) = \frac{\sinh(\sqrt{p}e_2)}{\sinh(\sqrt{p})} \tag{12}$$

3.1.2. ε^1 order identification. For ε^1 order, equations (9) yield

$$\begin{bmatrix} \theta_1(0) \\ 0 \end{bmatrix} = \begin{bmatrix} A_1 & B_1 \\ C_1 & D_1 \end{bmatrix}\begin{bmatrix} \theta_1^{\sup} \\ \Phi_1(e_1) \end{bmatrix} \tag{13a}$$

$$\begin{bmatrix} \theta_1^{\sup} \\ \Phi_1(e_1) \end{bmatrix} = \begin{bmatrix} \theta_1^{\inf} + I_0 \\ \Phi_1(e_1) \end{bmatrix} \tag{13b}$$

$$\begin{bmatrix} \theta_1^{\inf} \\ \Phi_1(e_1) \end{bmatrix} = \begin{bmatrix} A_2 & B_2 \\ C_2 & D_2 \end{bmatrix}\begin{bmatrix} \theta_1(1) \\ 0 \end{bmatrix} \tag{13c}$$

I_0 has the same definition as I in equation (9d), just replacing Ψ by Ψ_0. Substitution of Ψ_0 defined by equation (12), into this definition allows the calculation of integral I_0 and therefore the solution of set (13). The first order temperature on the rear face is given by

$$\theta_1(1) = -\frac{4}{\alpha\beta} K \frac{\sinh(ue_1)\sinh(\sqrt{p}e_2)}{\sinh(\sqrt{p})\sinh(u)} \tag{14}$$

where $K = \sin(\alpha\Delta_x/2)\cos(\alpha\Sigma_x/2)\sin(\beta\Delta_x/2)\cos(\beta\Sigma_x/2)$, $\Delta_q = q_2 - q_1$; $\Sigma_q = q_1 + q_2$, for $q = (x, y)$.

The front face temperature can be calculated in the same way [5, 9]. The product equation (14) and ε represents the Laplace–Fourier transform, $\Delta\theta = \varepsilon\theta_1$, of the contrast ΔT. The return to the original (t, x, y) domain can be achieved numerically by using Fast Fourier Transform (FFT) and Stehfest [26] algorithms. The analytical formula (14) is very simple even in this three-dimensional transient heat transfer situation. Simulations have been carried out to assess the effectiveness of this model. For the sake of clarity, only two-dimensional calculations have been performed. Figure 2 shows a comparison between the true contrast and the perturbed one at three different times for a small resistance $R_c = 0.01$. The perturbed contrast profiles are in excellent agreement with the true ones. However, for higher resistances ($R_c = 0.5$) the approximation is not adequate, confirming the restriction of the model to weak flaws (figure 3). Moreover, one can immediately realize that $\Delta\theta$ is linear in ε, which means that for small ε the contrasts produced by two discontinuities, for example, of resistances ε_1 and ε_2 located at distinct depths with different lateral extents (i.e. a multi-delamination in an impacted composite [9, 14]), simply add up. Nevertheless, this is not the case for the temperature. Indeed, this can be inferred from the Laplace temperature for two superimposed flaws:

$$\tau(x, y, 1, p) = \frac{\cosh(\sqrt{p})}{\sqrt{p}\sinh(\sqrt{p})}\{1 + \varepsilon_1 f_1 + \varepsilon_2 f_2\} + \mathrm{O}(\varepsilon) \tag{15}$$

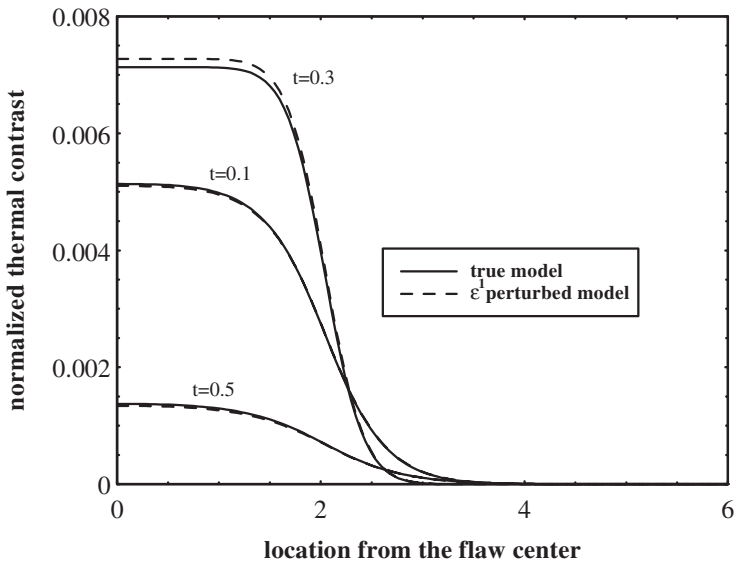

Figure 2. Comparison between the true model and the first order perturbed solution. The perturbation parameter is the thermal resistance, $\varepsilon = R_c$. Simulation parameters are $\varepsilon = 0.01$, $a = 4$, $b = \infty$, $e_1 = 0.5$, $L = 20$, $l = \infty$. The shown profiles correspond to three normalized times $t = 0.1$, 0.3 and 0.5.

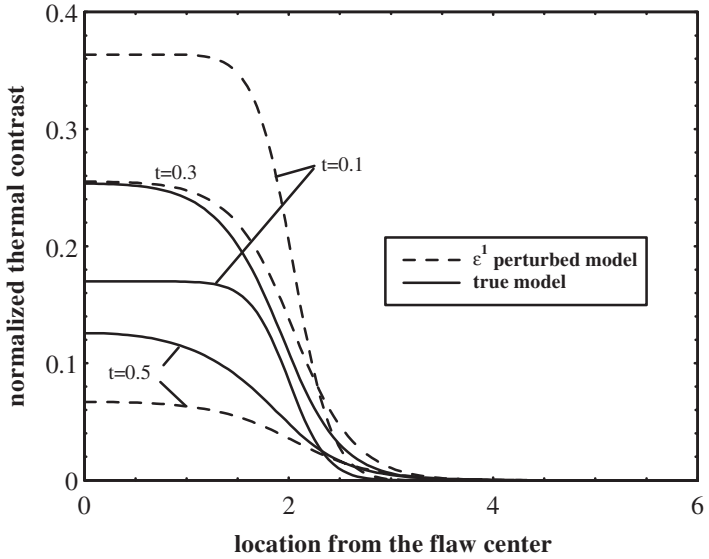

Figure 3. Comparison between the true model and the first order perturbed solution. The perturbation parameter is the thermal resistance, $\varepsilon = R_c$. Same parameter values as for figure 2 except that now $\varepsilon = 0.5$.

where $f_m(x, y, 1, p)$ is the inverse Fourier transform of $\theta_1(1)$ multiplied by $\sqrt{p}\sinh(\sqrt{p})$. The f_m function is written using the location parameters of the flaw number m ($m = 1, 2$). We note here that equation (15) can also be written by substituting, on its right hand-side, the term between braces by its [0, 1] Padé's approximant, namely $\{1 - \varepsilon_1 f_1 - \varepsilon_2 f_2\}^{-1}$. The $[N, M]$ Padé's approximant of a series $S(\varepsilon) = \sum_{n=0}^{\infty} c_n \varepsilon^n$ is the rational fraction in ε, with a numerator of degree N and a denominator of degree M, such that its expansion into a Taylor's series coincides with the series $S(\varepsilon)$ [21]. The use of Padé's approximant has the advantage of 'sticking' the solution to the true model for larger ε_m while being equivalent to equation (15) for small values of these parameters. Figure 4 illustrates how this correction reduces the deviation seen previously in figure 3 for high resistances ($R_c = 0.5$) between the true and perturbed models. For small values ($R_c = 0.01$), there is no difference between the true model and the Padé's approximant.

Another distinctive application of the contrast superposition property is the case of several flaws of very small sizes ($dx\,dy$) located at the same depth e_1. This can simulate a discontinuity of any shape, i.e. like a non-uniform adhesive layer. The coefficient K appearing in equation (14) is in this case given by

$$K = \frac{\alpha\beta}{4}\cos(\alpha x)\cos(\beta y)\,dx\,dy \tag{16}$$

Substitution of K into the equation leading to the resulting contrast yields

$$\begin{aligned}\Delta\theta(\alpha, \beta, 1, p) &= \int_0^L \int_0^l \varepsilon(x, y)\frac{\sinh(ue_1)\sinh(\sqrt{p}e_2)}{\sinh(\sqrt{p})\sinh(u)}\cos(\alpha x)\cos(\beta y)\,dx\,dy \\ &= \rho(\alpha, \beta)\frac{\sinh(ue_1)\sinh(\sqrt{p}e_2)}{\sinh(\sqrt{p})\sinh(u)}\end{aligned} \tag{17}$$

where $\rho(\alpha\beta)$ is the cosine spectrum of the contact resistance $\varepsilon(x, y)$. Equation (17) has been confirmed with a more general two-dimensional model valid for any value of a continuously non-uniform resistance $R_c(x)$ [9, 11–13, 15].

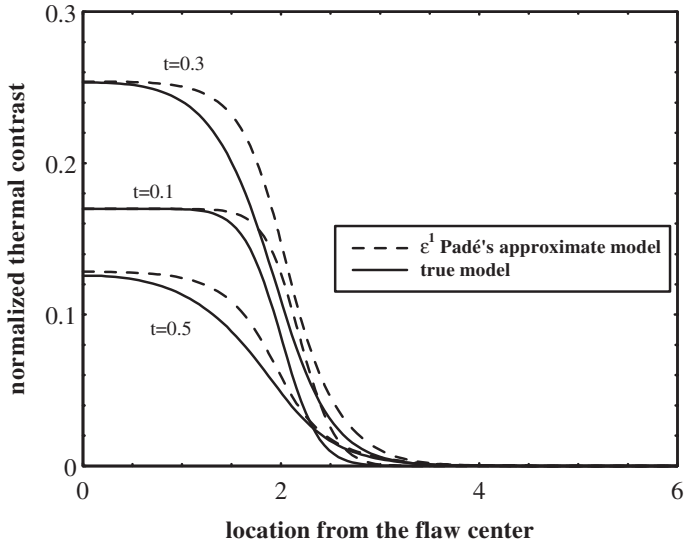

Figure 4. Comparison between the true model and the first order perturbed solution improved using Padé's approximant approach. The perturbation parameter is still the thermal resistance $\varepsilon = R_c$. Same parameter values as for figure 3.

3.2. Flaw of high resistance

The small parameter this time is the inverse of the contact resistance:

$$\eta = \frac{1}{R_c} \tag{18}$$

The new expansion series with respect to η are:

$$\theta(\alpha, \beta, z, p) = \sum_{i=0}^{\infty} \theta_i(\alpha, \beta, z, p)\eta^i \tag{19}$$

$$\Phi(\alpha, \beta, z, p) = \sum_{i=0}^{\infty} \Phi_i(\alpha, \beta, z, p)\eta^i \tag{20}$$

Introducing the new parameter η, the interface condition can be expressed in the Laplace domain as follows:

- temperature jump above the flaw,

$$\eta(\tau^{\sup} - \tau^{\inf}) = \psi(e_1) \tag{21}$$

- same temperature outside the flaw,

$$\tau^{\sup} = \tau^{\inf} \tag{22}$$

On the other hand, quadrupole equations (9*a*) and (9*c*) which describe heat diffusion in the upper and lower layers, keep the same structure. Hence, the formulation of the successive terms of the perturbation can be done the same way as for low resistances.

3.2.1. η^0 order identification. The perturbation of the interface condition leads to

- the first order heat flux is zero above the flaw, $\psi_0(e_1) = 0$
- same temperature outside the flaw, $\tau_0^{\sup} = \tau_0^{\inf}$.

This is the typical case of a homogeneous material containing a flaw of infinite resistance value. To solve the problem, we may assume that the heat flux is piecewise constantly distributed. The flux is zero above the flaw and is approximated by the flux in a flawless material elsewhere. This does not correspond to reality since at the flaw's edge, the interface flux is infinite and farther from it, it catches up to the level of a sound material. In spite of this, the η^0 order solution is determined taking into account this approximation, by adding up two new simpler problems:

(a) A sound medium subjected to a Dirac heat pulse

$$\begin{bmatrix} \theta_{0s}(0) \\ \dfrac{\sin(\alpha L)}{\alpha} \dfrac{\sin(\beta l)}{\beta} \end{bmatrix} = \begin{bmatrix} A_1 & B_1 \\ C_1 & D_1 \end{bmatrix} \begin{bmatrix} A_2 & B_2 \\ C_2 & D_2 \end{bmatrix} \begin{bmatrix} \theta_{0s}(1) \\ 0 \end{bmatrix} \tag{23}$$

The rear face temperature of the sound material is calculated as

$$\theta_{0s}(1) = \frac{1}{u \sinh(u)} \frac{\sin(\alpha L)}{\alpha} \frac{\sin(\beta l)}{\beta} \tag{24}$$

where the subscript 's' indicates the sound specimen.

(b) A source of heat flux set at the interface cancels the flux generated in a sound material above the flaw and keeps it unchanged elsewhere:

$$\psi_{0s}(e_1) = -\frac{\sinh(\sqrt{p}e_2)}{\sinh(\sqrt{p})} \qquad \text{above the flaw(area } \Omega_{af}) \tag{25}$$

$$\psi_{0s}(e_1) = 0 \qquad \text{outside the flaw (area } \Omega_{of}) \tag{26}$$

Two fully independent quadrupole relationships are thus obtained for the upper and lower layer:

$$\begin{bmatrix} \theta_{0h}(0) \\ 0 \end{bmatrix} = \begin{bmatrix} A_1 & B_1 \\ C_1 & D_1 \end{bmatrix} \begin{bmatrix} \theta_{0h}^{sup} \\ \displaystyle\iint_{\Omega_{af}} \Psi_{0s}(e_1) \cos(\alpha x) \cos(\beta y)\, dx\, dy \end{bmatrix} \tag{27}$$

$$\begin{bmatrix} \theta_{0h}^{inf} \\ \displaystyle\iint_{\Omega_{af}} \Psi_{0s}(e_1) \cos(\alpha x) \cos(\beta y)\, dx\, dy \end{bmatrix} = \begin{bmatrix} A_2 & B_2 \\ C_2 & D_2 \end{bmatrix} \begin{bmatrix} \theta_{0h}(1) \\ 0 \end{bmatrix} \tag{28}$$

where the subscript 'h' corresponds to the heat flux set at the depth flaw.

The combination of the two last equations yields the rear face temperature:

$$\theta_{0h}(1) = -\frac{\sinh(\sqrt{p}e_2)}{\sinh(\sqrt{p})} \frac{1}{u \sinh(ue_2)} \frac{4K}{\alpha\beta} \tag{29}$$

K is given by equation (14). The η^0 order component of the rear face temperature is then determined by adding $\theta_{0s}(1)$ and $\theta_{0h}(1)$.

3.2.2. η^1 order identification. The quadrupole relationships in this case are

$$\begin{bmatrix} \theta_1(0) \\ 0 \end{bmatrix} = \begin{bmatrix} A_1 & B_1 \\ C_1 & D_1 \end{bmatrix} \begin{bmatrix} \theta_1^{sup} \\ \Phi_1(e_1) \end{bmatrix} \qquad \text{for the upper layer} \tag{30}$$

$$\begin{bmatrix} \theta_1^{inf} \\ \phi_1(e_1) \end{bmatrix} = \begin{bmatrix} A_2 & B_2 \\ C_2 & D_2 \end{bmatrix} \begin{bmatrix} \theta_1(1) \\ 0 \end{bmatrix} \qquad \text{for the lower layer} \tag{31}$$

Starting from equation (21), we can calculate the first order Fourier flux at the flaw depth using equations (27) and (28) by

$$\phi_1(e_1) = \theta_{0h}^{sup}(e_1) - \theta_{0h}^{inf}(e_1) \tag{32}$$

Then, based on equations (31) and (32), the first order component of the rear face temperature is obtained by

$$\theta_1(1) = \frac{\sinh(u)\sinh(\sqrt{p}e_2)}{u^2\sinh(ue_1)\sinh^2(ue_2)\sinh(\sqrt{p})}\frac{4K}{\alpha\beta} \tag{33}$$

The rear face temperature can be approximated as follows:

$$\theta(\alpha, \beta, 1, p) = [\theta_{0s}(1) + \theta_{0h}(1)] + \eta\theta_1(1) + O(\eta) \tag{34}$$

Finally, the η^1 order contrast is obtained by subtracting the sound material temperature $\theta_{0s}(1)$ from the rear temperature $\theta(\alpha, \beta, 1, p)$:

$$\Delta\theta(\alpha, \beta, 1, p) = -\frac{\sinh(\sqrt{p}e_2)}{\sinh(\sqrt{p})u\sinh(ue_2)}\left(1 - \eta\frac{\sinh(u)}{u\sinh(ue_1)\sinh(ue_2)}\right)\frac{4K}{\alpha\beta} + O(\eta) \tag{35}$$

Similarly to the perturbation carried out for the case of small resistances, approximation (33) can be modified using a [0, 1] Padé's approximant to widen its validity field to medium resistances:

$$\Delta\theta(\alpha, \beta, 1, p) = -\frac{\sinh(\sqrt{p}e_2)}{\sinh(\sqrt{p})u\sinh(ue_2)}\frac{1}{1 + \eta(\sinh(u)/u\sinh(ue_1)\sinh(ue_2))}\frac{4K}{\alpha\beta} + O(\eta) \tag{36}$$

By substituting η by ε in the above equation, we can observe that it is equivalent to equation (14) corresponding to the ε first order perturbation when the resistance is very small. This formula is, therefore, very practical since it is useful for both high and weak contact resistances. However, it does not show how accurate the approximation is for medium values of R_c. For that reason, simulations have been performed for many values of the resistance. Figure 5 shows the

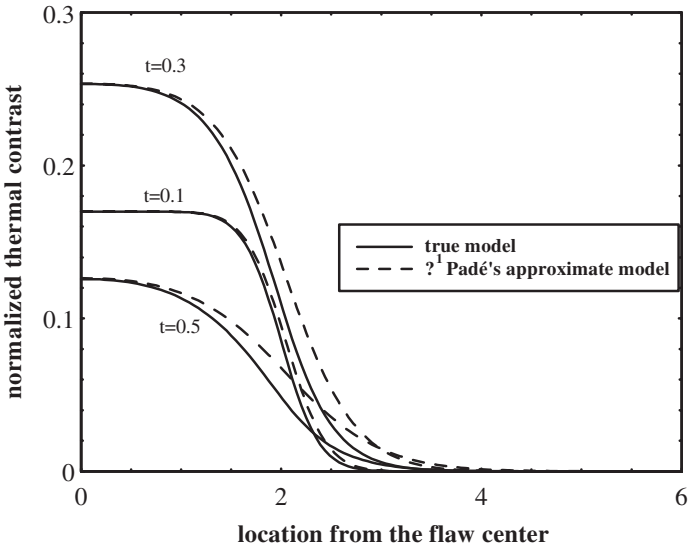

Figure 5. Comparison between the true model and the first order perturbed solution improved using Padé's approximant approach. The perturbation parameter is the thermal conductance, $\eta = 1/R_c$. Same parameter values as for figure 4.

robustness of the approximation for medium R_c values ($R_c = 0.5$). This model identifies the shape of the true contrast profiles better than the one illustrated in figure 4, in particular for short times ($t = 0.1$). Computational simulations showed that the true and the approximate curves never coincide, even for higher resistances. This was expected since in the model, we have assumed that the heat flux is piecewise constantly distributed (equations (23)–(26)). On the other hand, calculations for low resistances led to perfectly superimposed profiles. This new approach is, therefore, very practical for carrying out fast computational trials, since it gives a good approximation to real three-dimensional cases.

4. Conclusions

Unsteady three-dimensional heat diffusion within an anisotropic material containing a finite flaw has been solved, using a perturbation expansion and integral transforms. The perturbation method (first order only) has been used to achieve a simple and fast approximation. The two first order perturbations developed here are only valid when the resistance ($\varepsilon = R_c$) or the conductance ($\eta = 1/R_c$) are very small. For higher values of these parameters, many components in the perturbed series are needed for the algorithm to converge. Consequently, the analytical formulation becomes very complex and the calculation time too long. Furthermore, the perturbation method loses its advantages when compared to the traditional numerical methods approach. An improvement of the first order solutions has been obtained by using the Padé's approximant method. This formalism allows to widen the validity of the first order perturbed solution for higher values of the perturbing parameter. Simulations have shown that the reduced models are in a good agreement with the true solution for any value of the thermal resistance. The true solution is obtained by solving a linear set of equations whose unknowns are the Fourier components of the heat flux density at the flaw depth. The perturbation formalism has also led to simple analytical solutions that describe heat diffusion throughout superimposed flaws and a continuously non-uniform interface.

In conclusion, the results obtained in this work show the usefulness of the perturbation approach in the solution of problems that are difficult to solve by traditional means. The simplicity of the formulation, the short processing times and the possibility to perform an effortless sensitivity analysis of the parameters of interest, speak in favour of this approach.

References

[1] Vavilov V 1992 Thermal nondestructive testing: short history and state of the art *Quantitative Infrared Thermography Conf. (Châtenay-Malabry, France)* pp 179–89

[2] Beck J V, Blackwell B and St Clair C R Jr 1985 *Inverse Heat Conduction* (New York: Wiley)

[3] Tikhonov A N and Arsenin V Y 1977 *Solutions of Ill-posed Problems* (Washington, DC: Winston)

[4] Alifanov O M 1994 *Inverse Heat Transfer Problems* (Berlin: Springer)

[5] Batsale J C, Bendada A, Maillet D and Degiovanni A 1993 Distribution of a thermal contact resistance: inversion using experimental Laplace and Fourier transformations and an asymptotic expansion *Inverse Problems in Engineering: Theory and Practice Conf. (Palm Coast, Florida)* pp 139–46

[6] Ramos F M 1992 Résolution d'un problème inverse multidimensionnel de diffusion par la méthode des éléments analytiques et par le principe de l'entropie maximale: contribution à l'identification des défauts internes *Thesis of Ecole Nationale Supérieure de l'Aéronautique et de l'Espace* France

[7] Krapez J C, Maldague X and Cielo P 1991 Thermographic NDE: data inversion procedures: Part II. 2D analysis and experimental results *Res. Nondestructive Evaluat.* **3** 101–24

[8] Houlbert A S, Lamine A S and Degiovanni A 1991 Modélisation d'un défaut limité en vue du contrôle non destructif des matériaux anisotropes *Int. J. Heat and Mass Transfer* **34** 1125–38

[9] Bendada A 1995 Tomographie Infrarouge Stimulée: estimation d'une résistance d'interface non uniforme *Thesis of Institut National Polytechnique de Lorraine* France

[10] Batsale J C, Maillet D and Degiovanni A 1994 Extension de la méthode des quadripôles thermiques à l'aide de transformations intégrales—calcul du transfert thermique au travers d'un défaut plan bidimensionnel *Int. J. Heat and Mass Transfer* **37** 111–27

[11] Bendada A, Maillet D, Batsale J C and Degiovanni A 1998 Reconstruction of a non-uniform interface thermal resistance by inverse conduction *Inverse Prob. Eng. J.* **6** 79–123

[12] Bendada A, Batsale J C, Degiovanni A and Maillet D 1994 Interface resistances: the inverse problem for the transient thermal technique *Inverse Prob. Eng. Mech.* ed Bui, Tanaka *et al* (Rotterdam: Balkema) pp 347–54

[13] Bendada A, Batsale J C, Maillet D and Degiovanni A 1994 Estimation de la répartition spatiale d'une résistance thermique d'interface par méthode inverse *Thermique et Energétique à travers la Science et l'Industrie Conf. (Paris, France)* pp 4–10

[14] Bendada A, Maillet D and Degiovanni A 1992 Nondestructive transient thermal evaluation of laminated composites: discrimination between delaminations thickness variations and multidelaminations *Quantitative Infrared Thermography Conf. (Châtenay-Malabry, France*) pp 218–23

[15] Degiovanni A, Bendada A, Batsale J C and Maillet D 1994 Analytical simulation of a multi-dimensional temperature field produced by planar defects of any shape: application to non destructive testing *Quantitative Infrared Thermography Conf. (Sorrento, Italy*) pp 253–9

[16] Degiovanni A 1988 Conduction dans un Mur Multicouche avec Sources: Extension de la Notion de Quadripôles *Int. J. Heat and Mass Transfer* **31** 553–7

[17] Aziz A and Na T 1984 *Perturbations Methods in Heat Transfer* (Berlin: Springer)

[18] Hagen K D 1987 A solution to unsteady conduction in periodically layered composite media using a perturbation method *J. Heat Transfer* **109** 1021–3

[19] Nayfeh A H 1973 *Perturbation Methods* (New York: Wiley)

[20] Shanks D 1955 Nonlinear transforms of divergent and slowly convergent series *J. Math. Phys.* **34** 1–42

[21] Baker G A 1965 The theory and application of Padé approximant method *Advances in Theoretical Physics* (New York: Academic Press) 1–58

[22] Maillet D, Philippi I, Bendada A and Degiovanni A 1998 Integral transforms and parameter estimation in diffusive transfer *Inverse Problems in Engineering: Theory and Practice Conference (Le Croisic, France)* pp 463–71

[23] Cotta R M 1994 The integral transform method in computational heat and fluid flow *The 10th International Heat Ttransfer Conf. (Brithon, UK)* vol 1, Keynote papers, Special keynote (SK-3) pp 43–60

[24] Maillet D, Batsale J C, Bendada A and Degiovanni A 1996 Integral methods and non-destructive testing through stimulated infrared thermography *Revue Générale de Thermique* **35** 14–27

[25] Leturcq Ph, Dorkel J M, Ratolojanarhary F E and Tounsi S 1993 A two-port network formalism for 3D heat conduction analysis in multilayered media *Int. J. Heat and Mass Transfer* **36** 2317–26

[26] Stehfest H 1970 Remarks on Algorithm 368, Numerical Inversion of Laplace Transforms *Com A C M* 624